

Preparation, characterization and As(V) adsorption behaviour of CNT-ferrihydrite composites

Gérrard Eddy Jai Poinern¹, D. Parsonage¹, Touma B. Issa¹, M.K. Ghosh², E. Paling³ and P. Singh^{1,*}

¹ Faculty of Minerals and Energy, Murdoch University, Murdoch, WESTERN AUSTRALIA 6150

² Institute of Minerals and Materials Technology, Bhubaneswar 751013, INDIA

³ School of Environmental Sciences, Murdoch University, Murdoch, WESTERN AUSTRALIA 6150

*Corresponding author Email: P.Singh@murdoch.edu.au

Abstract

A Carbon nano tube (CNT)–Ferrihydrite nanocomposite was synthesized through precipitation in ethyl alcohol media. Its detailed characterization was carried out using XRD, SEM, FTIR and EDAX. The adsorption characteristics of the composite for As(V) removal were carried out as function of pH, adsorbent dose, As(V) concentration and contact time. Although pure CNT did not show any significant adsorption, CNT-Ferrihydrite proved to be a good adsorbent for arsenic. With increase in pH, the As(V) adsorption on the composite first decreased up to pH 5.0, thereafter it remained nearly constant. The adsorption followed the Langmuir isotherm model and from the data its monolayer adsorption capacity was estimated to be 44.1 mg/g. The adsorption data were best described by the pseudo-second order kinetic model.

Keywords: Carbon nanotubes, ferrihydrite, arsenic, adsorption, isotherms

1. Introduction

Serious ground water environmental problem posed by arsenic both from natural and anthropogenic sources has become a global concern because arsenic is highly toxic and carcinogenic to man and other living organisms. Similarly waste liquors of some metallurgical industries which contain higher concentration of arsenic than in contaminated ground waters also pose a major problem for safe disposal. Several techniques for removing arsenic from such solutions are currently used. The most common methods involve oxidation-precipitation, coagulation-precipitation, adsorption, ion-exchange and membrane filtration. Adsorption is the most favoured technique due to its simplicity of operation and economic considerations. Mohan and Pittman (2007) have carried out an exhaustive review of this subject.

Carbon nanotubes (CNT) due to their unique structures and exceptional properties have been the focus of research and development since their discovery in 1991 (Iijima, 1991). Their thermal and chemical stabilities have made them attractive adsorbents for organic and inorganic contaminants in water (Li *et al.*, 2002; Peng *et al.*, 2003).

Due to their large specific area, CNTs are also suitable for using as support material for various composite materials. Li *et al.* (2001) deposited amorphous Al₂O₃ using carbon nano tubes as supports and showed that (Al₂O₃/CNT) composite had almost four times higher fluoride adsorption capacity than γ -Al₂O₃. Peng *et al.* (2005) prepared iron oxide - CNT magnetic composites and used for removal of Pb(II) and Cu(II) from water. They showed that after adsorption the adsorbent could be separated from the medium by a simple magnetic process with >98% recovery. CNT alone or its composites with other material have not been previously investigated for the remediation of arsenic from water. Synthetic ferrihydrite and other iron oxides/hydroxides as well as those which occur naturally are known to play an important role in the sequestration of contaminants from ground water through adsorption (Schwertmann and Taylor, 1989). Ferrihydrite has previously been studied for its use in arsenic remediation from water (Raven *et al.*, 1998; Jia and Demopoulos, 2005).

The objective of the present work is to investigate the ability of CNT to remove arsenic from contaminated water by adsorption. A CNT-ferrihydrite composite has also been included in the work to establish how the composite material performs for removal of arsenic from aqueous media. The potential of CNT and the CNT-ferrihydrite composite for arsenic removal has been determined

by carrying out batch adsorption studies. A relatively high arsenic concentration (up to 100 mg/L) has been used keeping in view the treatment option of hydrometallurgical waste solutions.

2. Experimental

2.1 CNT

CNT were obtained from NanoAmor Nanostructured & Amorphous Materials Inc. Houston, TX, USA. The tubes had an outer diameter of 20-50nm, length of less than 2 μ m and a purity of approximately 95%.

2.2 Ferrihydrite-CNT composite

A 250mL solution of 0.1M iron (III) nitrate solution was prepared by dissolving Fe(NO₃)₃·9H₂O in absolute ethanol. CNT (0.05 g) were added to the solution and dispersed by ultrasonication at 80% intensity for 30 minutes. This solution was then homogenized with a homogenizer at 15000rpm and tetraethyl ammonium hydroxide (TEAH) was added drop-wise via a burette, until the pH reached 9. The solution was continually stirred for a further 5 minutes to ensure completion of the reaction. The solution was filtered under vacuum and the precipitate was washed thoroughly with ultrapure water to remove any excess reagent. The precipitate was then dried in a vacuum desiccator for 48 hours after which it was crushed to a consistent fine powder with a mortar and pestle and stored in a sealed sample vial.

2.3 Characterization

The surface areas of the adsorbents before and after arsenic loading were determined by the BET method at the Commonwealth Scientific and Industrial Research Laboratory, Bentley, Western Australia. The structure and morphological features of the adsorbents were investigated with a high resolution field emission scanning electron microscope (Zeiss 1555 VP-FESEM) at 3kV with a 30 μ m aperture under 1 x 10⁻¹⁰ Torr pressure.

EDAX data were collected using SiLi line scanning detector attached to a scanning electron microscope. The system resolution was 105eV with an accelerating voltage of 20.0kV. The scan was over a range 0.0 to 14.0 keV. The data was analyzed using the ISIS-EDX software.

Fourier transform infrared spectroscopy was performed in Thermo Scientific Nicolet 6700 FTIR spectrometer by scanning KBr discs of the samples in the range 400 – 3500 cm⁻¹. The data was analyzed using the OMNIC software.

X-Ray Diffraction spectra were recorded with a Siemens D500 series diffractometer using Cu K α = 1.5406 Å radiation, 40kV and 30 mA. The diffraction spectra were collected at room temperature over the 2 θ range 20° to 80° at 0.04° step size, with an acquisition time of 2 seconds.

2.4 Adsorption studies

The As(V) solutions of required concentrations were prepared by diluting appropriate volumes of a stock solution. The pH of solutions was adjusted by adding 0.1M HNO₃ or 0.1M NaOH as required. The adsorption studies were carried out by placing known volumes of the various As(V) solutions in contact with pre determined amounts of the adsorbents in tightly closed bottles. The bottles were subjected to shaking for the required period of time by placing them in a Perth Scientific shaking water bath at 75 rpm at 25°C. After shaking, the suspension was filtered twice using a 0.22 μ m Millipore syringe filter unit and the filtrate was analyzed for residual arsenic by ICP-MS at the NATA accredited Marine and Freshwater Research Laboratory (MAFRL), Murdoch University.

3 Results and discussion

3.1 Characterization of CNT and CNT-ferrihydrite composite

The surface area of CNT, as determined by the BET method was found to be 129.3m²/g. The surface area of the CNT-Ferrihydrite composite was 231.6m²/g indicating the synthesized composite had a much higher surface area (almost double) than the CNT used in the experiment. Figure 1(a) shows the FESEM image of the CNT. The material consisted of regular tube structures of length <2 μ m, with outer diameter in the range 30-50 nm. The FESEM image of CNT-ferrihydrite composite (Fig.1 (b)) shows that the material consisted of CNT covered with agglomerated ferrihydrite particles with bundle like structure. In some regions, the CNT's appeared to remain separated from the ferrihydrite. Thus the composite was a two phase solid.

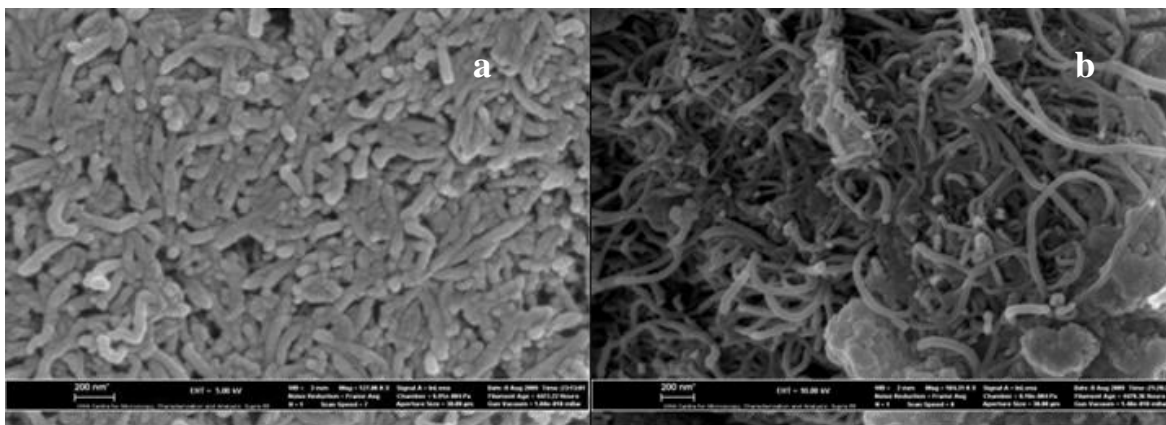


Figure 1. FESEM images of (a) CNT and (b) CNT-ferrihydrate composite

Figure 2 (a) displays the X-Ray diffraction pattern of CNT which shows that the main crystal orientation (h k l) was (002) corresponding to 2θ value of 26.1° . The XRD pattern is consistent with that reported by Emmanuel, *et al.* (2009) and Gao, *et al.* (2004).

In the XRD pattern of CNT-ferrihydrate composite [Figure 2 (b)], two broad peaks at around 35° and 62° are visible. Overall, the XRD pattern resembles that of the 2-Line ferrihydrate. (Kukkadapu *et al.*, 2004 ; Schwertmann and Cornell, 1991).

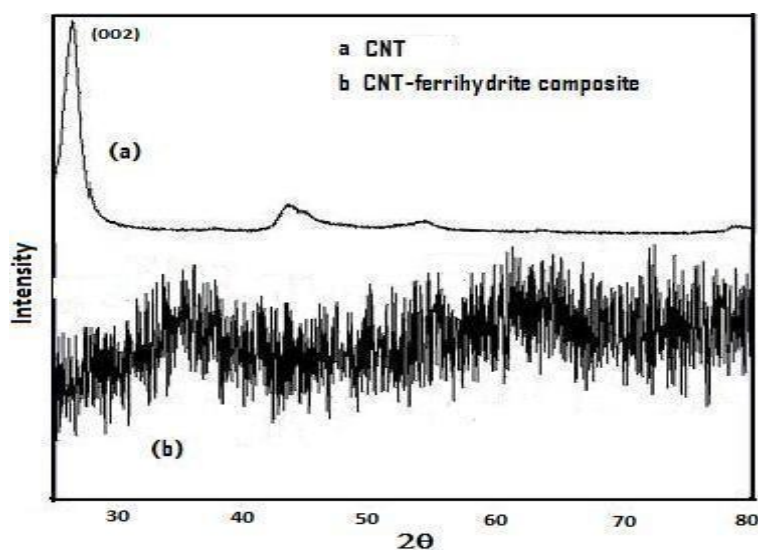


Figure 2. XRD patterns of (a) MWCNT and (b) CNT-ferrihydrate composite.

The FTIR spectrum of the CNT-ferrihydrate is displayed in Figure 3. The near infrared region has peaks at 472.6 , 587.2 and 665.2cm^{-1} , which are characteristic of Fe-O bonds (Liu *et al.*, 2009). The band at 2881 and the shoulder at 2942cm^{-1} can be attributed to the symmetrical and asymmetrical stretching of the $-\text{CH}_2-$. The prominent band at $\sim 3000\text{cm}^{-1}$ is assigned to the asymmetrical stretching of $-\text{CH}_3$, whereas the symmetrical and asymmetrical bending vibrations of $-\text{CH}_3$ are located at ~ 1361 and $\sim 1482\text{cm}^{-1}$ respectively. The prominent band at 1740cm^{-1} is distinctive of carbon nanotube vibrational modes. The bands at 1580 and 2357cm^{-1} correspond to C-O bonds (Jiang *et al.*, 2003; Misra *et al.*, 2006), which arise from the carbonate contamination resulting from the atmospheric carbon dioxide reacting with ferrihydrate (Liu *et al.*, 2009). The band at 1676cm^{-1} is assigned to the O-H bending mode of water, whereas the other O-H stretching bands are in the region $3000-3400\text{cm}^{-1}$. The broad stretching of the bands in this region is due to adsorbed or lattice water (Liu *et al.*, 2009; Jia *et al.*, 2007; Kahani and Jafari, 2009).

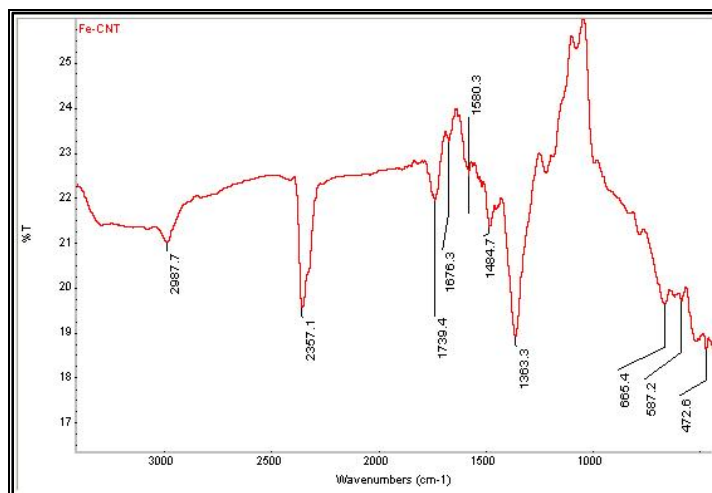


Figure 3. FTIR spectrum of CNT-ferrhydrite composite

3.2 Effect of initial pH on As(V) adsorption

The effect of pH, in the range 2-10, on adsorption of As(V) on CNT and CNT-ferrhydrite composite was investigated. The other parameters which were kept constant were: $[\text{As(V)}]_{\text{initial}}$ 50 mg/L, adsorbent concentration 1g/L, temperature 25⁰C and, contact time 2.5h. Figure 4 shows that pH variation had little effect on the As(V) adsorption on CNT and overall adsorption was very low (c.a. 3.8%). The lack of suitable functional groups on CNT would explain this observation. The ionic adsorption capability is known to be mainly determined by the functional groups which are usually introduced by chemical treatments such as oxidation (Dabrowski, 1999). Appropriate treatments can introduce functional groups such as hydroxyl (-OH), carboxyl (-COOH) and carbonyl (>C=O), on the surface of CNTs (Li *et al.*, 2002). Introduction of functional groups on CNT enhances its ionic adsorption properties.

Unlike the CNT used in this work, the arsenic adsorption on CNT-ferrhydrite composite is found to be highly pH dependent. As can be seen from Figure 4, the As (V) adsorption is high at pH 2 and decreases rapidly to pH 5 after which increase in pH does not have much effect. As(V) predominantly exists as H_2AsO_4^- and HAsO_4^{2-} in the pH range 2.7 to 11.5 (Tripathy and Raichur, 2008). Acidic solutions provide sufficient protonated sites to the adsorbent which result in a net positively charged surface. Negatively charged oxyanions are attracted to these sites.

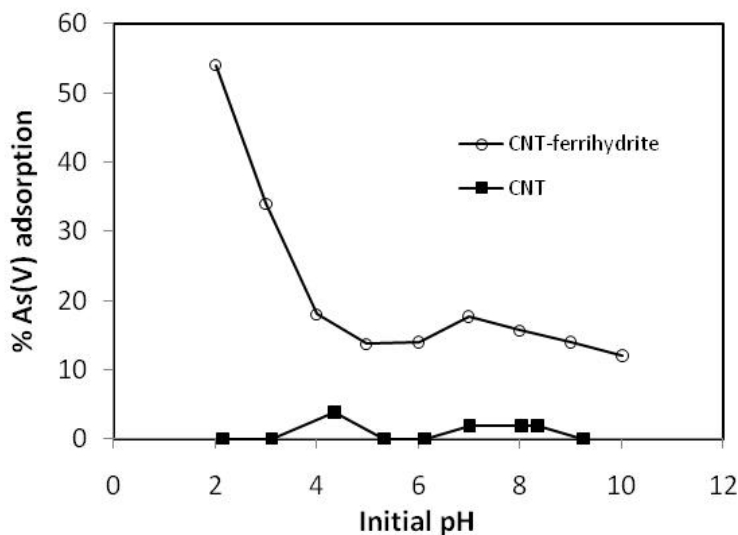


Figure 4. Effect of initial pH on As(V) adsorption on CNT and CNT-ferrhydrite composite. [Conditions: 298 K, adsorbent dose 1g/L, contact time 2.5 h, initial As(V) 50mg/L]

At high pH the adsorbent surface is negatively charged through adsorption of hydroxyl ions leading to repulsive forces between the negatively charged surface and oxyanions. Since adsorption is favoured in acidic media (pH<5) this material should be a

valuable reagent for arsenic remediation from acidic hydrometallurgical waste liquors. Thus further adsorption studies were carried out at pH 3.

3.3 Effect of adsorbent dose on As(V) adsorption

The effect of CNT-Ferrihydrite composite dose in the range 1 g/L to 10 g/L on As(V) adsorption was investigated at pH 3. The initial As(V) concentration was kept constant at 50 mg/L and the contact time used was 2.5 h. Figure 5 shows that the As (V) adsorption increased from 37% to 80 % when the adsorbent dose increased from 1 g/L to 10 g/L. The adsorption capacity decreased from 17.7 mg/g to 3.9 mg/g. The increase in % As(V) adsorption with the increase in adsorbent dose may be due to increased available adsorption sites and the decrease in adsorption capacity is mainly due to unsaturation of adsorption sites through adsorption reaction.

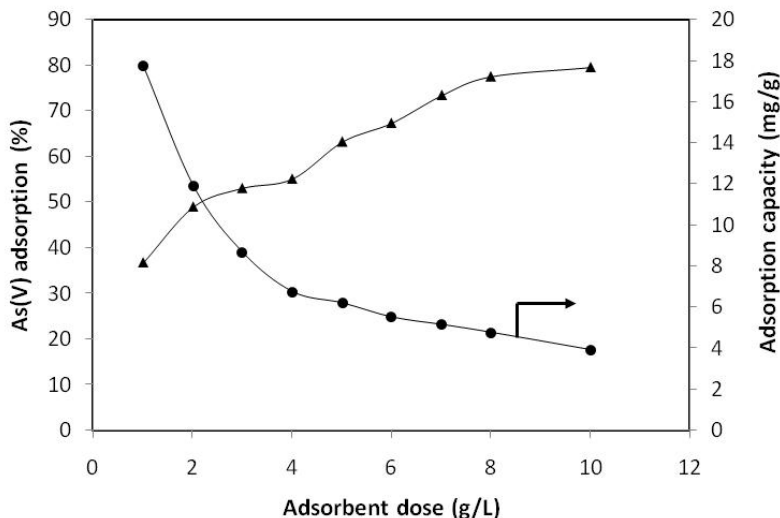


Figure 5. Effect of adsorbent dose on As(V) adsorption. [Conditions: 298 K, pH 3.0, contact time 2.5 h, initial As(V) 50mg/L]

3.4 Kinetics of As (V) adsorption on CNT-ferrhydrite

The kinetics of arsenic adsorption on CNT-ferrhydrite were determined under the conditions: initial arsenic concentration 50mg/L, pH 3, adsorbent dose 1 g/L and temperature 25°C. The contact time was varied from 15 minutes to 4 hours. The adsorption occurred in two phases: fast for about 90 minutes followed by a slower phase. The equilibrium was established in about 3 h. To ensure attainment of equilibrium, all further experiments were carried out to 4 h duration.

The experimental data were processed with respect to three different kinetic models namely pseudo-first order (Lagergren, 1898), pseudo-second order (McKay and Ho, 1999) and intra-particle diffusion (Weber and Morriss, 1963).

The equations (1) and (2) represent the linear forms of the pseudo-first order and pseudo-second order models respectively.

$$\log(q_e - q_t) = \log q_e - \frac{k_1}{2.303} t \quad (1)$$

$$\frac{t}{q_t} = \frac{1}{k_2 q_e^2} + \frac{1}{q_e} t \quad (2)$$

Where, q_e (mg/g) and q_t (mg/g) are amounts of As(V) adsorbed at equilibrium and at time t respectively. k_1 (/min) and k_2 (g/min.mg) are the pseudo-first order and pseudo-second order adsorption rate constant respectively.

Figure 6 and Figure 7 show pseudo-first order and pseudo-second order plots respectively for the experimental data. Various rate constants derived from the slopes and intercepts along with correlation coefficients are given in Table 1. The pseudo-second order plot (Figure 7) has better correlation coefficient (R^2). The calculated value of adsorption capacity from the plot in Figure 7 is found to be closer to the experimentally determined value than that calculated from Figure 6. This suggests that the pseudo-second order model represents the kinetic data more accurately.

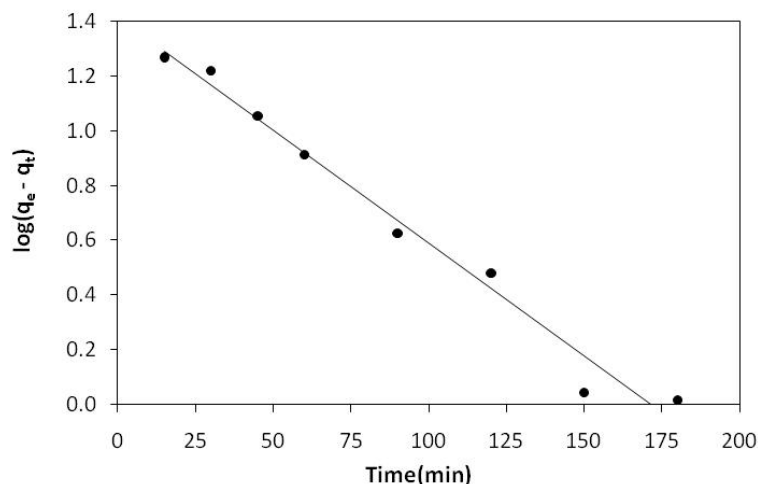


Figure 6. Pseudo-first order plot for As(V) adsorption on CNT-ferrihydrate. [Conditions: 298 K, adsorbent dose 1g/L, initial [As(V)] 50mg/L, pH 3]

Table 1. Rate constants and correlation coefficients for kinetic models

$q_{e,expt}$ (mg/g)	Pseudo-first order model			Pseudo-second order model			Intra-particle diffusion		
	$q_{e,cal}$ (mg/g)	k_1 (min^{-1})	R^2	$q_{e,cal}$ (mg/g)	k_2 (g/mg.min)	R^2	k_{id} (mg/g.min ^{1/2})	C (mg/g)	R^2
34.2	26.06	0.019	0.980	38.46	9.18×10^{-4}	0.997	2.72	4.23	0.978

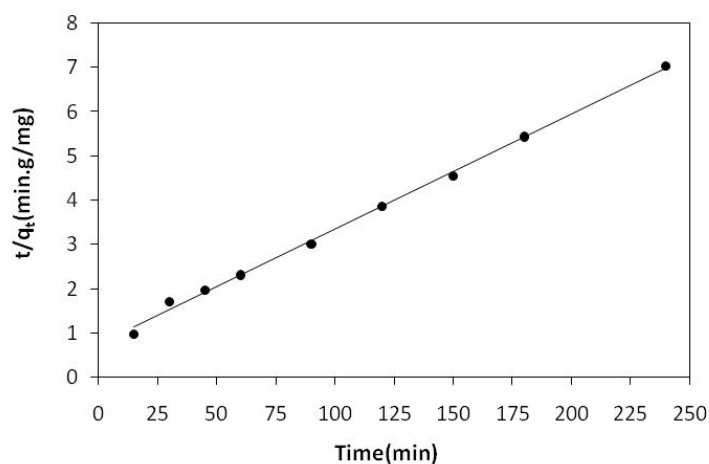


Figure 7. Pseudo-second order plot for As(V) adsorption on CNT-ferrihydrate. [Conditions: 298 K, adsorbent dose 1g/L, initial [As(V)] 50mg/L, pH 3]

The intra-particle diffusion model, proposed by Weber and Morris (1963), is expressed as

$$q_t = k_{id} \sqrt{t} + C \quad (3)$$

where, k_{id} is the intra-particle diffusion rate constant (mg/g.min^{1/2}) and C is a constant related to boundary layer thickness (mg/g).

If intra-particle diffusion is involved in the adsorption process, the $t^{1/2}$ versus q_t plot should be linear and should go through the origin if intra-particle diffusion is the sole rate-controlling step. Figure 8 shows that the plot of q_t vs. $t^{1/2}$ is not linear over the entire time period. This implies that more than one process is controlling the adsorption. The dotted line is indicative of the intra-particle

diffusion on the CNT-ferrihydrate, for which the rate constant and intercept are given in Table 1. It could be concluded from the results that intra-particle diffusion predominantly influences the rate during the first 90 minutes of the experiment. After this period equilibrium approaches and the adsorption slows down.

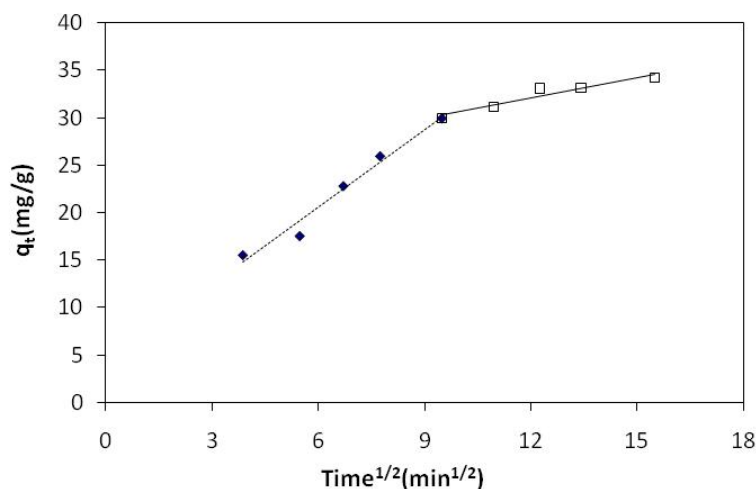


Figure 8. Intra-particle diffusion model plot for As(V) adsorption.
[Conditions: 298 K, adsorbent dose 1g/L, initial [As(V)] 50mg/L, pH 3]

3.5 Adsorption isotherms

The distribution of adsorbate between aqueous phase and adsorbent is a measure of the position of equilibrium in an adsorption process and can be investigated through various models such as the Langmuir and Freundlich isotherms. The Langmuir model is based on the assumption of homogeneous monolayer coverage with all sorption sites to be identical and energetically equivalent. The Freundlich model assumes physicochemical adsorption on heterogeneous surfaces. The linear forms of the two models are:

$$\text{Langmuir} \quad \frac{C_e}{q_e} = \frac{C_e}{Q_m} + \frac{1}{Q_m b} \quad (4)$$

$$\text{Freundlich} \quad \ln q_e = \ln K_F + \frac{1}{n} \ln C_e \quad (5)$$

where, C_e (mg/L) is equilibrium As(V) concentration in the solution, Q_m (mg/g) is the monolayer adsorption capacity, and b (L/mg) is the Langmuir adsorption constant related to the free energy of adsorption. K_F (mg/g)(mg/L)^{-1/n} and n (dimensionless) are Freundlich adsorption isotherm constants being indicative of extent of adsorption and intensity of adsorption, respectively.

The Langmuir isotherm equation was used to estimate the maximum adsorption capacity of the CNT-ferrihydrate composite under the conditions 298 K, pH 3.0, 4h contact time and 1 g/L adsorbent dose while varying initial As(V) concentration from 10 to 100 mg/L. The values of the isotherm constants and R^2 are given in Table 2. The linear plot (Figure 9) of C_e/q_e versus C_e along with high value correlation coefficient indicate that Langmuir isotherm provides a better fit with the equilibrium data.

The adsorption data when fitted to the Freundlich isotherm i.e. the plot of $\log q_e$ versus $\log C_e$ (Figure 10) shows that Freundlich isotherm gives a poor fit to the experimental data as compared to Langmuir isotherm. The isotherm parameters as derived from the slope and intercept of the plots are listed in Table 2.

The Langmuir monolayer capacity (mg/g) of CNT-ferrihydrate composite for arsenic adsorption is calculated to be 44.1 mg/g. This value is only slightly lower than that for pure ferrihydrate prepared by an identical method suggesting that the presence of CNT in the composite material has virtually no effect on arsenic adsorption. The arsenic removal efficiency of the CNT-ferrihydrate composite could be compared with those of other adsorbents by referring to the data in (Table 3). The data shows that CNT-ferrihydrate composite has arsenic removal capacity higher than most of the materials reported in the literature.

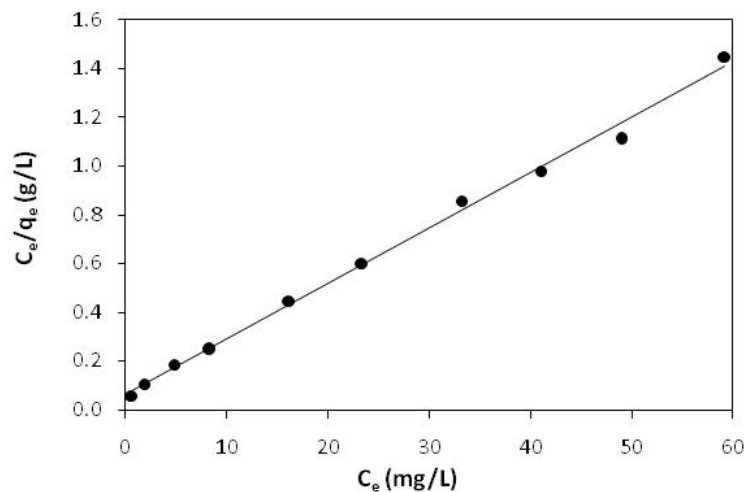


Figure 9. Langmuir isotherm plot of adsorption equilibrium data. [Conditions: 298 K, adsorbent dose 1g/L, contact time 4 h, pH 3.0]

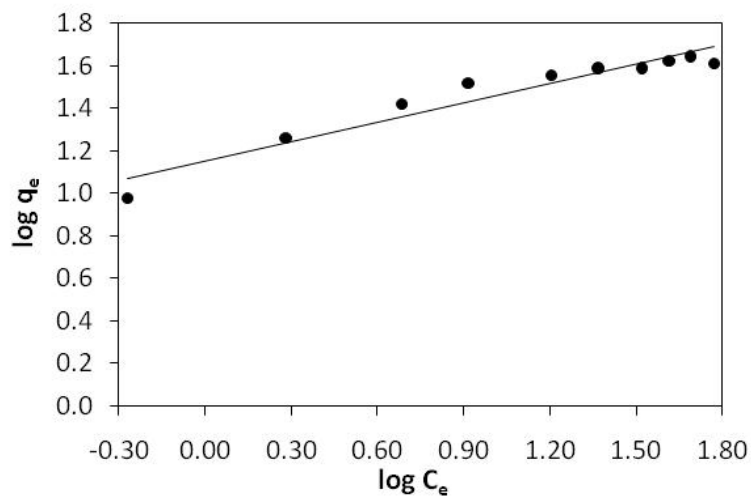


Figure 10. Freundlich isotherm plot of adsorption equilibrium data. [Conditions: 298 K, adsorbent dose 1g/L, contact time 4 h, pH 3.0]

Table 2. Langmuir and Freundlich isotherm constants

Isotherms	Constants/ Correlation coefficients	Values
Langmuir	R^2	0.996
	Q_m	44.1 mg/g
	b	0.347 L/mg
Freundlich	R^2	0.927
	K_F	14.17
	n	3.305

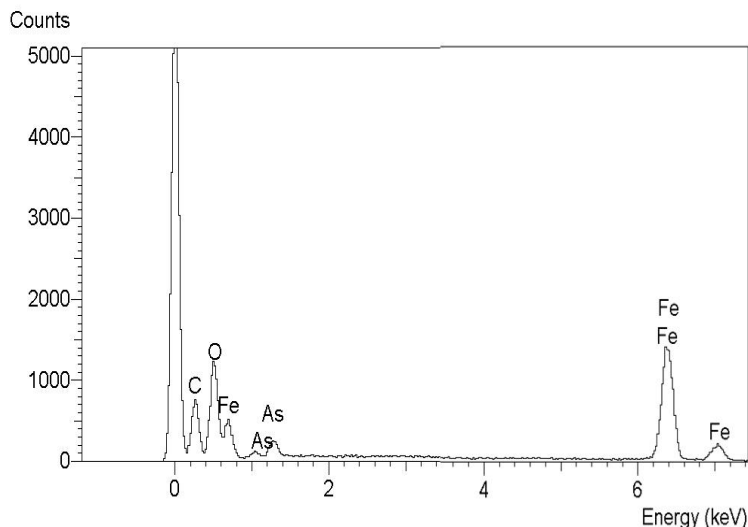


Figure 12. EDAX microanalysis of arsenic loaded CNT-ferrihydrate sample

4. Conclusion

From the foregoing studies the following conclusions are drawn

1. A CNT-ferrihydrate composite has been synthesised by precipitation technique using a Fe(III) salt solution in alcohol as a solvent and tetraethyl ammonium hydroxide as the reagent for hydroxide ions.
2. The surface area of the composite compared to the CNT used in the preparation is very high.
3. It consists of CNT particles coated with agglomerates of ferrihydrate.
4. While CNT itself is a poor adsorbent for As(V), the composite is an excellent adsorbent and unlike CNT the adsorption on the composite is pH dependent. The adsorption decreases as the pH is increased from 2 to 5 after which it levels out. This property of the composite adsorbent would make it a valuable adsorbent for arsenic remediation from acidic hydrometallurgical waste liquors.
5. The adsorption closely follows the Langmuir adsorption isotherm indicating that monolayer adsorption mechanism occurs. The adsorption capacity as estimated from the Langmuir isotherm is 44.1 mg/g which is much higher than that reported for most commonly used adsorbents.
6. Kinetic data are consistent with the pseudo-second order model. The intra-particle diffusion plays a role in the rate controlling mechanism at least in the initial stages of adsorption.

Nomenclature

b	Langmuir equilibrium constant related to affinity, L/mg
C	constant related to boundary layer thickness, mg/g
C_e	Equilibrium As(V) concentration in the solution, mg/L
k_1	Pseudo-first order rate constant, /min
k_2	Pseudo-second order rate constant, g/mg.min
K_F	Freundlich adsorption isotherm constant, (mg/g)(mg/L) ^{-1/n}
k_{id}	Intra-particle diffusion rate constant, mg/g.min ^{1/2}
Q_m	monolayer adsorption capacity, mg/g
q_t	Adsorption capacity at any time t, mg/g
q_e	Adsorption capacity at equilibrium, mg/g
n	Freundlich isotherm constant related to intensity of adsorption

Acknowledgement

The authors acknowledge the financial support for this work through the Australia-India Strategic Research Fund. One of the authors (MKG) gratefully acknowledges the Visiting Research Fellowship offered by Murdoch University, Australia.

References

- Altundoğan, H.S., Altundoğan, S., Tümen, F. and Bildik, M., 2000. Arsenic removal from aqueous solutions by adsorption on red mud. *Waste Management*, Vol. 20, pp. 761-767.
- Bhakat, P.B., Gupta, A.K., Ayoob, S., and Kundu, S., 2006. Investigations on As(V) removal by modified calcined bauxite. *Colloids and Surfaces A*, Vol. 281, pp. 237- 245.
- Chutia, P., Kato, S., Kojima, T. and Satokawa, S., 2009. Arsenic adsorption from aqueous solution on synthetic zeolites. *Journal of Hazardous Materials*, Vol. 162, pp. 440-447.
- Deliyanni, E.A., Bakoyannakis, D.N., Zouboulis, A.I. and Matis, K.A., 2003. Sorption of As(V) ions on akaganeite-type nanocrystals. *Chemosphere*, Vol. 50, pp. 155-163.
- Gupta, K., Saha, S. and Ghosh, U.C., 2008. Synthesis and characterization of nanostructure hydrous iron-titanium binary mixed oxide for arsenic sorption. *Journal of Nanoparticle Research*, Vol. 20, pp. 1361-1368.
- Dabrowski, A., 1999. *Adsorption and its Applications in Industry and Environmental Protection*. Amsterdam, Elsevier.
- Emmanuel, B., Thomas, S., Raghuvaran, G. and Sherwood, D., 2009. Simulated XRD profiles of carbon nanotubes (CNTs): An efficient algorithm and a recurrence relation for characterising CNTs. *Journal of Alloys and Compounds*, Vol. 479, No. 1-2, pp. 484-488.
- Gao, X.P., Zhang, Y., Chen, X., Pan, G.L., Yan, J., Wu, F., Yuan, H.T. and Song, D.Y., 2004. Carbon nanotubes filled with metallic nanowires. *Carbon*, Vol. 42, No. 1, pp. 47-52.
- Iijima, S., 1991. Helical microtubes of graphitic carbon. *Nature*, Vol. 354, No.7, pp. 56-58.
- Jia, Y., Demopoulos, G.P., 2005. Adsorption of arsenate onto ferrihydrite from aqueous solution: Influence of media (sulfate vs nitrate), added gypsum, and pH alteration. *Environmental Science and Technology*, Vol. 39, pp. 9523-9527.
- Jia, Y., Xu, L., Wang, X., Demopoulos, G.P., 2007. Infrared spectroscopic and X-ray diffraction characterisation of the nature of adsorbed arsenate on ferrihydrite. *Geochimica et Cosmochimica Acta*, Vol. 71, No. 7, pp. 1643-1654.
- Jiang, L., Gao, L., Sun, J., 2003. Production of aqueous colloidal dispersions of carbon nanotubes. *Journal of Colloid and Interface Science*, Vol. 260, No. 1, pp. 89-94.
- Kahani, S.A., Jafari, M., 2009. A new method of preparation of magnetite from iron oxyhydroxide or iron oxide and ferrous salt in aqueous solution. *Journal of Magnetism and Magnetic Materials*, Vol. 321, No. 13, pp. 1951-1954.
- Kukkadapu, R.K., Zachara, J.M., Fredrickson, J.K. and Kennedy, D.W., 2004. Biotransformation of two-line silica-ferrihydrite by a dissimilatory Fe(III)-reducing bacterium: Formation of carbonate green rust in the presence of phosphate. *Geochimica et Cosmochimica Acta*, Vol. 68, No. 13, pp. 2799-2814.
- Lagergren, S., 1898. Zur theorie der sogenannten adsorption gelöster stoffe. *Kungliga Svenska Vetenskapsakademiens Handlingar*, Vol. 24, pp. 1-39.
- Li, Y.H., Wang, S., Cao, A., Zhao, D., Zhang, X., Xu, C., Luan, Z., Ruan, D., Liang, J., Wu, D. and Wei, B., 2001. Adsorption of fluoride from water by amorphous alumina supported on carbon nanotubes. *Chemical Physics Letters*, Vol. 350, No.5-6, pp. 412-416.
- Li, Y.H., Wang, S., Wei, J., Zhang, X., Xu, C., Luan, Z., Wu, D., Wei, B., 2002. Lead adsorption on carbon nanotubes. *Chemical Physics Letters*, Vol. 357, No. 3-4, pp. 263-266.
- Li, Y.H., Xu, C., Wei, B., Zhang, X., Zheng, M., Wu, D., Ajayan, P.M., 2002. Self-organised Ribbons of Aligned Carbon Nanotubes. *Chemistry of Materials*, Vol. 14, pp. 483-485.
- Liu, H., Li, P., Lu, B., Wei, Y., Sun, Y., 2009. Transformations of ferrihydrite in the presence or absence of trace Fe(II): The effect of preparation procedures of ferrihydrite. *Journal of Solid State Chemistry*, Vol. 182, No. 7, pp. 1767-1771.
- McKay, G. and Ho, Y.S., 1999. Pseudo-second order model for sorption processes. *Process Biochemistry*, Vol. 34, pp. 451-465.
- Misra, A., Tyagi, P.K., Singh, M.K., Misra, D.S., 2006. FTIR studies of nitrogen doped carbon nanotubes. *Diamond and Related Materials*, Vol. 15, No. 2-3, pp. 385-388.
- Mohan, D. and Pittman, C.U., 2007. Arsenic removal from water/wastewater using adsorbents – A critical review. *Journal of Hazardous Materials*, Vol. 142, pp. 1-53.
- Mohapatra, D., Mishra, D. and Park, K.H., 2008. A laboratory scale study on arsenic(V) removal from aqueous medium using calcined bauxite ore. *Journal of Environmental Sciences*, Vol. 20, pp. 683-689.
- Park, H., Myung, N.V., Jung, H. and Choi, H., 2009. As(V) remediation using electrochemically synthesized maghemite nanoparticles. *Journal of Nanoparticle Research*, Vol. 11, pp. 1981-1989.
- Peng, X., Li, Y.H., Luan, Z., Di, Z., Wang, H., Tian, B. and Jia, Z., 2003. Adsorption of 1,2-dichlorobenzene from water to carbon nanotubes. *Chemical Physics Letters*, Vol. 376, No. 1-2, pp. 154-158.
- Peng, X., Luan, Z., Di, Z., Zhang, Z. and Zhu, C., 2005. Carbon nanotubes-iron oxides magnetic composites as adsorbent for removal of Pb(II) and Cu(II) from water. *Carbon*, Vol. 43, No. 4, pp. 880-883.
- Raven, K.P., Jain, A. and Loeppert, R.H., 1998. Arsenite and arsenate adsorption to ferrihydrite: Kinetics, equilibrium and adsorption envelopes. *Environmental Science and Technology*, Vol. 32, pp. 344-349.
- Schwertmann, U. and Cornell, R.M., 1991. *Iron Oxides in the Laboratory: Preparation and Characterization*. Weinheim, VCH Verlagsgesellschaft mbH.

- Schwertmann, S. and Taylor, R.M., 1989. Iron oxides. *Minerals in Soil Environments*, ed. J.B. Dixon, Weed, S.B., Madison, Wisconsin: Soil Science Society of America.
- Tripathy, S.S. and Raichur, A.M., 2008. Enhanced adsorption capacity of activated alumina by impregnation with alum for removal of As(V) from water. *Chemical Engineering Journal*, Vol. 138, pp. 179-186.
- Tuutijärvi, T., Lu, J., Sillanpää, M. and Chen, G., 2009. As(V) adsorption on maghemite nanoparticles. *Journal of Hazardous Materials*, Vol. 166, pp. 1415-1420.
- Weber, W.J.J. and Morris J.C., 1963. Kinetics of adsorption on carbon from solution. *Journal of Sanitary Engineering Division of American Society of Civil Engineers*, Vol. 89, pp. 31-60.

Biographical notes

Gérrard Eddy Jai Poinern holds Ph.D. from Murdoch University Western Australia. He is a Senior Lecturer in Physics & Nanotechnology, and Director of Murdoch Applied Nanotechnology Research Group, Murdoch University. His research interests include: Nanoparticles for use in environmental cleanup, nanoparticles in photovoltaics, production of nanorods and nanotubes. Application of nanotechnology in the areas of drug delivery and medical treatment such as in nerve repair, stroke treatment and skin burns.

Dale Parsonage holds B.Sc. from Murdoch University, Western Australia.

Touma B. Issa holds Ph.D. from Murdoch University, Western Australia. He is the Chief Chemist of ZBB Technologies Ltd, Australia and Adjunct Research Associate at Murdoch University. His research interests include: Analytical Chemistry particularly relating to atmospheric pollution, Electrochemistry as applied to batteries, Waste water purification and remediation of ground drinking water.

Malay Kumar Ghosh holds Ph.D. in Chemical Engineering from Indian Institute of Technology, Kharagpur. He is a scientist at the Department of Hydro and Electrometallurgy, Institute of Minerals and Materials Technology, Bhubaneswar, India. His research interests include: Leaching, precipitation, waste treatment and hydrometallurgical pilot plants.

Eric Paling holds Ph.D. from University of Western Australia. He is an Associate Professor at Murdoch University and is the Director of the Marine and Freshwater Laboratory. His research interests include: Seagrass dynamics and rehabilitation; Mangrove assessment on arid coasts; Marine nutrient cycling and processes in water, plants and sediment; Aerial assessment of macrophytes.

Pritam Singh holds Ph.D. from Murdoch University, Western Australia. He is an Emeritus Professor at Murdoch University. His research interests include: General Electrochemistry, Corrosion, Metal Electrodeposition, Electrometallurgy, Zinc-bromine Battery, Lead-acid and Lithium Batteries, Arsenic Remediation from Ground Drinking Water and Mineral Wastes.

Received July 2010

Accepted October 2010

Final acceptance in revised form October 2010